ENCIT 2018

ABCM Associação Brasileira de Engenharia e Ciências Mecânicas

17th Brazilian Congress of Thermal Sciences and Engineering
November 25th-28th, 2018, Águas de Lindóia, SP, Brazil

ENCIT-2018
Computational Simulation of Turbulent Flow and Heat Transfer of Supercritical CO_2 in a Micro Modular Reactor (MMR) Subchannel

Carolina S. B. Dutra
Nuclear Engineering Department - POLI/UFRJ: Av. Horacio Macedo, 2030/G206, Rio de Janeiro, RJ
cdutra@poli.ufrj.br

Felipe P. Ribeiro
Jian Su
Nuclear Engineering Program - PEN/UFRJ: Av. Horacio Macedo, 2030/G206, Rio de Janeiro, RJ
felipeportor@poli.ufrj.br
sujian@nuclear.ufrj.br

Abstract. *In this work we present and analyze the steady-state thermal-hydraulic behavior of the supercritical CO_2 through of the computational modeling of the triangular arrayed rod bundle subchannel of the KAIST (Korea Advanced Institute of Science and Technology) MMR. The mathematical model was composed of the Reynolds–averaged Navier–Stokes equations (RANS), with the k-ω SST (Shear Stress Transport) turbulence model for the coolant fluid in the subchannel and the heat conduction equation for the fuel and cladding. The thermodynamic properties of CO_2 were implemented from National Institute of Standards and Technology (NIST) data. The transport equations were solved using a commercial CFD (Computational Fluid Dynamics) tool, ANSYS Fluent. Initially, a geometric model was constructed, using the ICEM software, composed of fuel, gap, cladding, coolant and two adiabatic regions of the fuel rod. It was performed a mesh sensitivity study and the study of the flow in the subchannel. Variation of mass flow rate showed the behavior of friction factor and Nusselt number as a function of the Reynolds number, demonstrating the use of different well-know frictional factor correlations for supercritical CO_2 flows.*

Keywords: *CFD (Computational Fluid Dynamics), Supercritical CO_2, Micro Modular Reactor*

1. INTRODUCTION

With the growth in energy demand, studying and optimizing energy production processes has increasingly become important. Currently, the supercritical carbon dioxide (CO_2) power cycle is considered as one of the most promising electric power generation systems due to its high efficiency, making CO_2 an excellent coolant for Micro Modular Reactors (MMRs).

To understand the thermodynamic properties of supercritical CO_2, several experimental analysis and numerical simulations have been carried out. Duffey and Pioro (2005) compared several published experimental works on the heat transfer of CO_2 flowing in vertical and horizontal circular tubes. Fatima (2010) investigated the thermo-hydraulic behavior of supercritical fluids in semicircular horizontal tubes. Kim and Kim (2010) and Bruch *et al.* (2009) quantified the heat transfer phenomenon of a supercritical fluid using an experimental facility of upward flow in a vertical tube. Bovard *et al.* (2017) investigated computationally the effect of fluid acceleration and buoyancy on the heat transfer coefficient of supercritical CO_2 and water in a vertical tube.

This work aims to analyze the steady-state behavior of the supercritical CO_2 by computational modeling of a triangular arrayed rod bundle of the KAIST (Korea Advanced Institute of Science and Technology) MMR (Yu *et al.*, 2015). The mathematical model is composed of the Reynolds-averaged Navier−Stokes equations (RANS), with the k-ω SST (Shear Stress Transport) turbulence model for the coolant fluid in the subchannel and the heat conduction equation for the fuel and cladding. The transport equations are solved by using a commercial CFD (Computational Fluid Dynamics) code, ANSYS Fluent. The thermodynamic properties of CO_2 are provided by the National Institute of Standards and Technology (NIST) data available in Fluent.

2. METHODS AND MATHEMATICAL MODELS

2.1 Equations

The mathematical model consists of the Reynolds averaged, Navier-States equations:

- Continuity equation

$$\frac{\partial \rho}{\partial t} + \bigtriangledown \cdot (\rho \vec{u}) = 0, \tag{1}$$

where ρ is density (kg/m^3), t is time (s) and u is velocity (m/s).

- Momentum equation

$$\frac{\partial \rho u_i}{\partial t} + \bigtriangledown \cdot (\rho u \vec{u}) = - \bigtriangledown p + \bigtriangledown \cdot \vec{\vec{\tau}} + \rho \vec{g}, \tag{2}$$

where g is gravity (m/s^2), p is pressure (Pa) and τ is the shear stress (Pa).

- Energy equation

$$\frac{\partial \rho e}{\partial t} - \frac{\partial p}{\partial t} + \bigtriangledown \cdot (\rho \vec{u} e) = - \bigtriangledown \cdot (k \bigtriangledown T) - p \bigtriangledown \vec{u} + \Phi + q''', \tag{3}$$

where k is the thermal conductivity (W/m K), e is the total energy (W/kg), T is the temperature (K), S_E is the entropy (J/K kg) and Φ is the volumetric source (-).

- State equation

$$\rho = \rho(P, T) \tag{4}$$

The heat generation in the fuel rod was given by the following correlation:

$$\dot{Q} = N \langle \dot{q} \rangle = NL \langle q' \rangle = NL\pi D_{co} \langle q''_{co} \rangle = NL\pi R_f^2 \langle q''' \rangle , \tag{5}$$

where N is the number of rods, L is the active height (m), q is the rate of energy generated in a pin (W/s), q' is the linear heat generation rate (W/m), q''_{co} is the surface heat flux (W/m^2), q''' is the volumetric heat generation rate (W/m^3), R_f is the fuel radius (m) and D_{co} is the external diameter of the rod (m).

2.2 Turbulence Model

The turbulence model used was the k$-\omega$ SST (Menter, 1994; Wilcox, 2008), which was chosen due to its ability to capture adequately the flow behaviour close to the wall. It is a two equations hybrid model that solves the flow near the wall by the k$-\omega$ model and the free flow region by the k$-\epsilon$ model. Therefore, besides being generally more stable it is better for general applications, justifying its choice. Its equations are essentially derived from Reynolds-averaged Navier-Stokes equations (RANS) and can be described as it follows (Vieira, 2014).

Turbulence kinetic energy, k:

$$\frac{\partial k}{\partial t} + \overline{u_j} \frac{\partial k}{\partial x_j} = \frac{\partial}{\partial x_j} \left[\left(\nu + \nu_t \left(\frac{1}{F_1^{-1} \sigma_{k1}} + \frac{1}{(1 - F_1)^{-1} \sigma_{k2}} \right) \right) \frac{\partial k}{\partial x_j} \right] + P_k \frac{\partial \overline{u_i}}{\partial x_j} - \beta_k k \omega, \tag{6}$$

Specific dissipation rate, ω:

$$\begin{aligned} \frac{\partial \omega}{\partial t} + \overline{u_j} \frac{\partial \omega}{\partial x_j} = \frac{\partial}{\partial x_j} \left[\left(\nu + \nu_t \left(\frac{1}{F_1^{-1} \sigma_{\omega 1}} + \frac{1}{(1 - F_1)^{-1} \sigma_{\omega 2}} \right) \right) \frac{\partial \omega}{\partial x_j} \right] \\ + (1 - F_1) \frac{2}{\sigma_{\omega 2} \upsilon} \left(\frac{\partial k}{\partial x_j} \frac{\partial \omega}{\partial x_i} \right) - \left[F_1 \beta_{\omega 1} + (1 - F_1) \beta_{\omega 2} \right] \omega^2 + \left[F_1 \alpha_1 + (1 - F_1) \alpha_2 \right] \frac{\omega}{k} P_k, \end{aligned} \tag{7}$$

where

$$P_k = \nu_t \left(\frac{\partial \overline{u_i}}{\partial x_j} + \frac{\partial \overline{u_j}}{\partial x_i} \right) - \frac{2}{3} \kappa \delta_{ij}, \tag{8}$$

and the turbulence viscosity is given by

$$\nu_t = \frac{\alpha k}{\max(\alpha\omega, SF_2)}, \tag{9}$$

where S is an invariant measure of strain rate.

2.3 Thermophysical Properties of the Materials

The mathematical model is solved numerically by using Fluent. The modeled subchannel is composed of fuel, gap, cladding and coolant, the latter being composed of CO_2. The CO_2 properties are a determining factor for a correct analysis of the thermal-hydraulic behavior. The CFD code used allows these properties to be introduced by several ways: as constant or variable values, through tables or correlations programmed in C language. However, its library contains the REFPROP (Reference fluid properties) tool developed by NIST and enabled by an User-defined function (UDF), providing properties for simulations with real gases. The present work makes use of this technique, not only for the CO_2, but also for the helium (He), which constitutes the gap of the fuel rod. The properties of the cladding (Todreas and Kazimi, 1990), made of zircalloy, were considered constant, using values for density, specific heat and thermal conductivity of 7200 kg/m^3, 330 J/kgK and 13 W/mK, respectively. For the fuel, constituted of Uranium Mononitride (UN), the value introduced for the density was 13550 kg/m^3. The thermal conductivity was given by a correlation (Takahashi *et al.*, 1971):

$$ks = 1.37T^{0.41}, \tag{10}$$

where T is the temperature of the material and was implemented by an UDF. Specific heat at constant pressure was implemented using the values shown in Table 1 and are calculated by the code using linear interpolation. It is important to mention that this fuel has a high melting temperature around 3078K.

Table 1. Specific heat at constant pressure of the UN fuel (Ross *et al.*, 1988).

Temperature (K)	300	400	500	600	700	800	900	1000
Cp (J/kg K)	190.11	204.55	213.35	220.16	225.97	231.12	236.1	240.75

3. PROPERTIES OF THE SUPERCRITICAL CO_2

When the temperature and pressure of a substance are both greater than their respective critical values, it is defined as supercritical fluid. The transition of the CO_2, for example, to the supercritical phase occurs at values of 7.38 MPa and 30.98^{o}C (304.13K).

By observing the graphs of thermodynamic properties (NIST, 2017), such as density, thermal conductivity, viscosity and specific heat, it is seen that these properties change rapidly as the critical point gets closer. Additionally, these properties tend to stabilize both with increasing temperature and pressure.

Due to the difficulty of finding exact values for the thermodynamic properties of the CO_2 immediately prior to the critical point, all the simulations were performed with temperatures higher than 304.5K.

4. RESULTS AND DISCUSSIONS

To analyze the behavior of CO_2 in a MMR, a subchannel of a triangular arrayed rod bundle was created. The geometry of this model, as well as the mesh, are presented below.

4.1 Geometric model

The geometric model, constructed by using the ICEM software, represents an interior subchannel of a triangular arrayed rod bundle with a central fuel rod and is composed of nuclear fuel, gap, cladding, coolant and two domains inside the rod without heat generation. Its dimensions are presented in Table 2 and its configuration, in Figure 1, according to the proposal for the KAIST MMR reactor model of Yu *et al.* (2015).

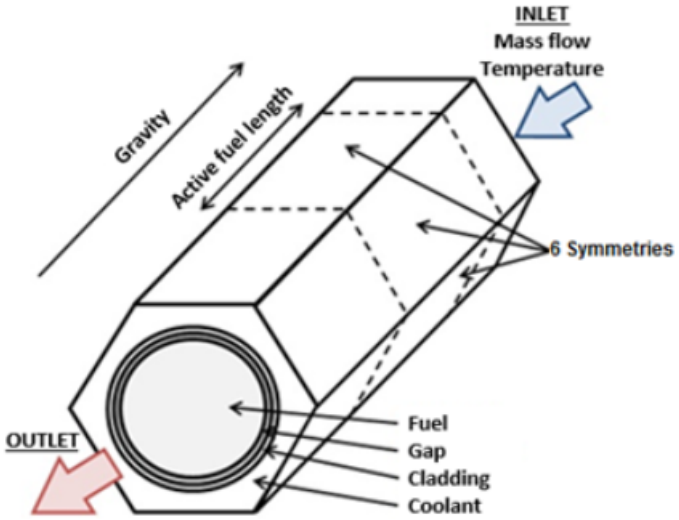

Figure 1. Simulation domain and boundary conditions.

Table 2. Fuel assembly design parameters of the KAIST MMR (Yu *et al.*, 2015).

Fuel radius (m)	0.69 x 10^{-2}
Gap radius (m)	0.7 x 10^{-2}
Cladding radius (m)	0.75 x 10^{-2}
Pitch (m)	1.695 x 10^{-2}
Axial dimensions of the fuel (m)	0.4 / 1.2 (active) / 1.2
Active height (m)	1.2

4.2 Mesh sensitivity study

After a mesh convergence analysis, the mesh with the best compromise between precision and computational cost was chosen. Seven meshes were tested, all of those were refined for values of the near wall grid spacing $(\Delta y+)$ less than 1, ensuring that there was an adequate treatment of boundary layer effects caused by viscosity. Those simulations were done isothermally, without needing to solve the Energy equation and with constant CO_2 properties.

Table 3. Mesh sensitivity study.

Mesh Number	Number of nodes	Pressure Drop (MPa)
Mesh 01	376134	0.019715
Mesh 02	670814	0.024511
Mesh 03	1036662	0.026541
Mesh 04	1473678	0.027535
Mesh 05	1981862	0.027972
Mesh 06	2561214	0.028269
Mesh 07	3211734	0.028178

It can be observed that the mesh number 05 has an acceptable precision, of 10^{-3}, and a low computational cost in relation to the meshes with more elements, being, therefore, the one chosen for the simulations of the subchannel. In Figure 2, the cross section of this mesh is shown.

4.3 Simulations

Once the mesh calculation has converged, the study of the flow in the subchannel was continued using the typical operating conditions of a MMR reactor (Yu *et al.*, 2015), summarized in Table 4.

For the simulation, the subchannel was initialized cold, T = 655K, and, over the iterations, all its domains were heated due to volumetric heat generation in the fuel. This gradual heating process for the average outlet temperature of the coolant in the subchannel, until it reaches variations of 10^{-7}, chosen as the convergence criterion, is shown in Figure 3. Although the graph is only for the outlet temperature, the average temperatures in all of the domains presented the same

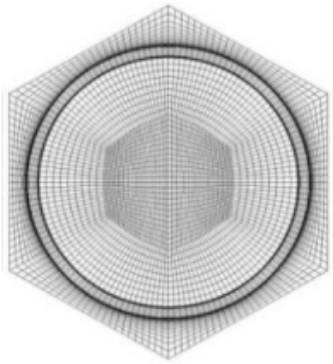

Figure 2. Cross section of the computational geometry and mesh details for Mesh 05.

Table 4. Bondary conditions.

Fluid pressure (MPa)	20
Inlet temperature (K)	655
Mass flow rate (kg/s)	0.0699579
Volumetric heat generation (kW/m^3)	8.45 x 10^7

behaviour. The calculated numerical results and those obtained by Yu *et al.* (2015). As the higher temperature achieved for the whole domain was 1292.25K for the fuel, it can be observed that the maximum temperature in each domain does not violate the safety conditions for a nuclear reactor, since the melting point for the fuel is not reached.

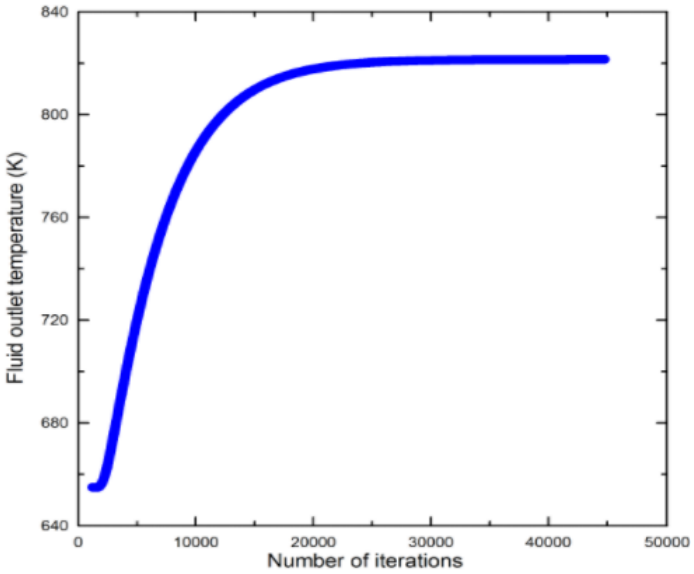

Figure 3. Convergence of the temperature in the fluid outlet.

The velocity and temperature fields in the cross sections at three different positions of the subchannel (Z =-1.0m, Z = 0m - center, and Z = 1.00m), are presented in Figure 4.

It is possible to observe that the velocity field increases along the cross-section with the increase of temperature, because of the expansion of the gas, and the smaller fluid velocity near the rod due to the friction with the wall. The coolant becomes hot because it removes the heat from the fuel rod. Therefore, the subchannel temperatures are higher the closer they are to the fuel, both axially and radially.

Afterwards, the mass flow rate was decreased, to vary the Reynolds number of the flow, the friction factor was also calculated through the Blasius correlation for Re < 30,000:

$$f = 0.316Re^{-0,25}, \tag{11}$$

where Re is the Reynolds number, and the McAdams relation for 30,000 < Re < 1,000,000:

$$f = 0.184Re^{-0,2}, \tag{12}$$

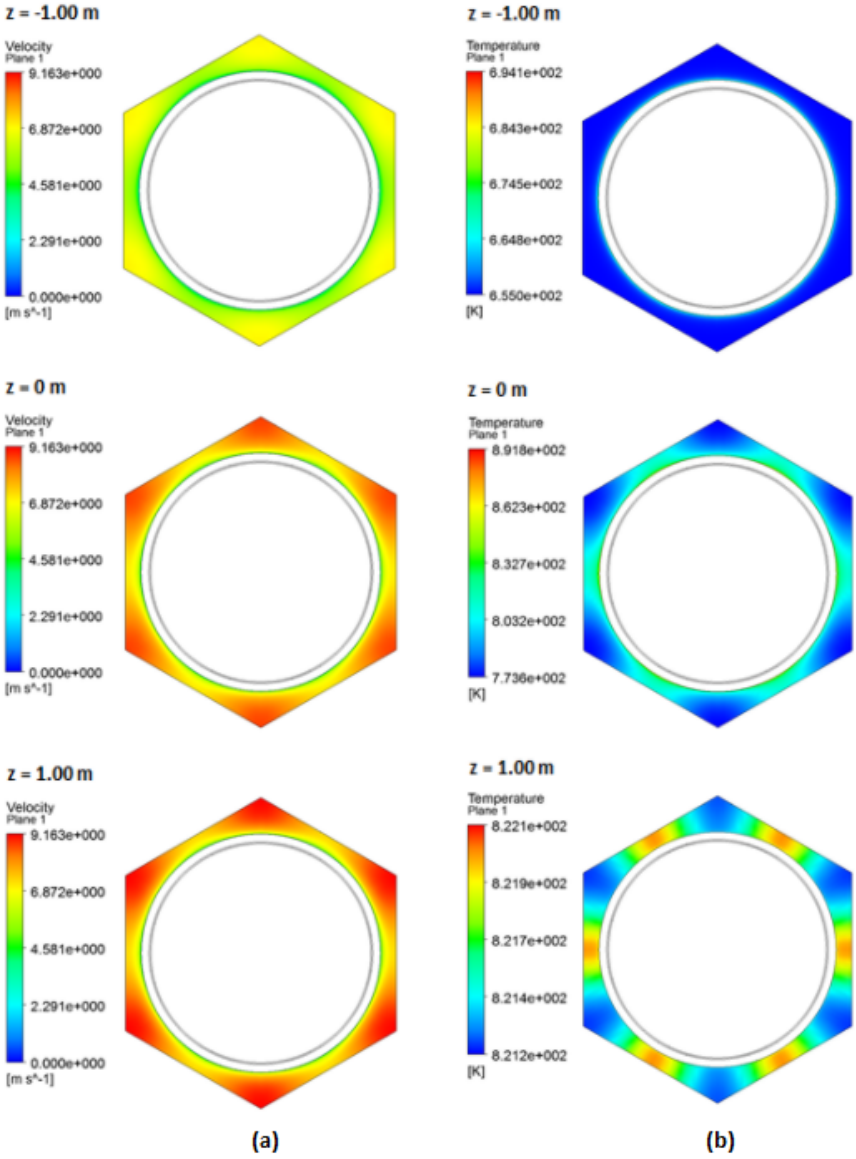

Figure 4. (a) Cross velocity fields in m/s (b) Cross temperature fields in K.

and also through the correlation for bare rod interior subchannel friction factor in hexagonal array (Todreas and Kazimi, 1990):

$$f \equiv \frac{C}{Re^n}, \tag{13}$$

where $n = 0.18$ for turbulent flow and

$$C = 0.1458 + 0.03632(P/D - 1) - 0.03333(P/D - 1)^2). \tag{14}$$

The friction factor was calculated using the wall shear stress, density and average velocity obtained by the simulations, using the formula:

$$f = \frac{8\tau_\omega}{\rho u^2}, \tag{15}$$

where τ_ω is the wall shear stress (in Pa).

As shown in Figure 5, the Reynolds number of the order of 10^4 confirms that the CO_2 in the present work has a turbulent behavior. It is possible to observe that for Re < 30,000, the friction factor calculated by the simulation agrees well with the Blasius correlation. For Re > 30,000, the curve calculated by CFD has the same shape as the curve of the McAdams correlation, but there is a static difference along her, which is understandable as McAdams correlation is a very

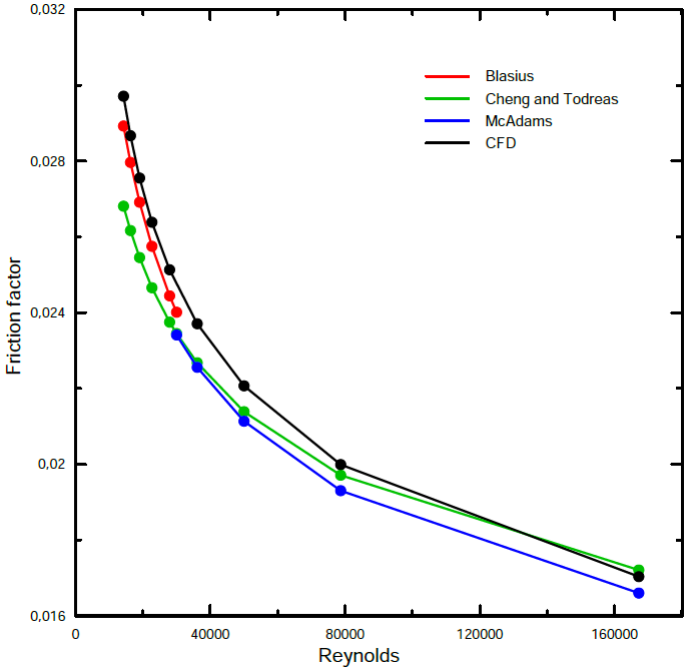

Figure 5. Friction factors as a function of Reynolds number, compared with empirical correlations.

general. On the other hand, for these higher Reynolds, the friction factor was best described by the Cheng and Todreas correlation, since it is a specific relation for the calculation of friction factors of bare rod interior subchannel in hexagonal array for turbulent flow.

Then, the influence of the Reynolds number on the heat transfer of the fuel active length was studied as indicated by the Nusselt number formula:

$$Nu = \frac{hD_H}{k} \tag{16}$$

The Nusselt number was calculated using the parameters obtained from the CFD simulation in seven different axial positions. Also, we estimated the Nusselt number using the Presser correlation (Todreas and Kazimi, 1990):

$$Nu = Nu_\infty \psi, \tag{17}$$

where,

$$Nu_\infty = 0.023 Re^{0.8} Pr^{0.4}, \tag{18}$$

and,

$$\psi = 0.9090 + 0.0783 \frac{P}{D} - 0.1283 e^{-2.4(\frac{P}{D}-1)}. \tag{19}$$

The comparison between the two calculated Nusselt numbers, as a function of the dimensionless axial position, is shown in Figure 6.

As can be seen, the curves of the two calculated Nusselts numbers are very similar. However, at the interface close to the non active fuel length they differ. This probably happened because there is a simulation numerical error, caused by the abrupt change in the boundary condition, that is the generation of heat. In Figure 7, it is possible to observe the Nusselt number of the last heated section of the active lenght as a function of Reynolds number. With this, it is possible to observe that the curves are very close and conclude that the Presser correlation describes our problem well.

5. CONCLUSION

The Blasius correlation for Re < 30,000 and the Cheng and Todreas for 30,000 < Re < 170,000 are able to represent well the supercritical CO_2 friction factor in a interior subchanel in a hexagonal array. While the Presser correlation allowed us to calculate the Nusselt Number, mainly near the last section of heated fluid, with extremely small errors in relation to what was calculated through numerical simulations.

It can be concluded that the numerical model developed at the present work well describes the thermal-hydraulic behavior of the CO_2 into a subchannel of a MMR, as well as the correlations used, even if they are not specific for supercritical fluids.

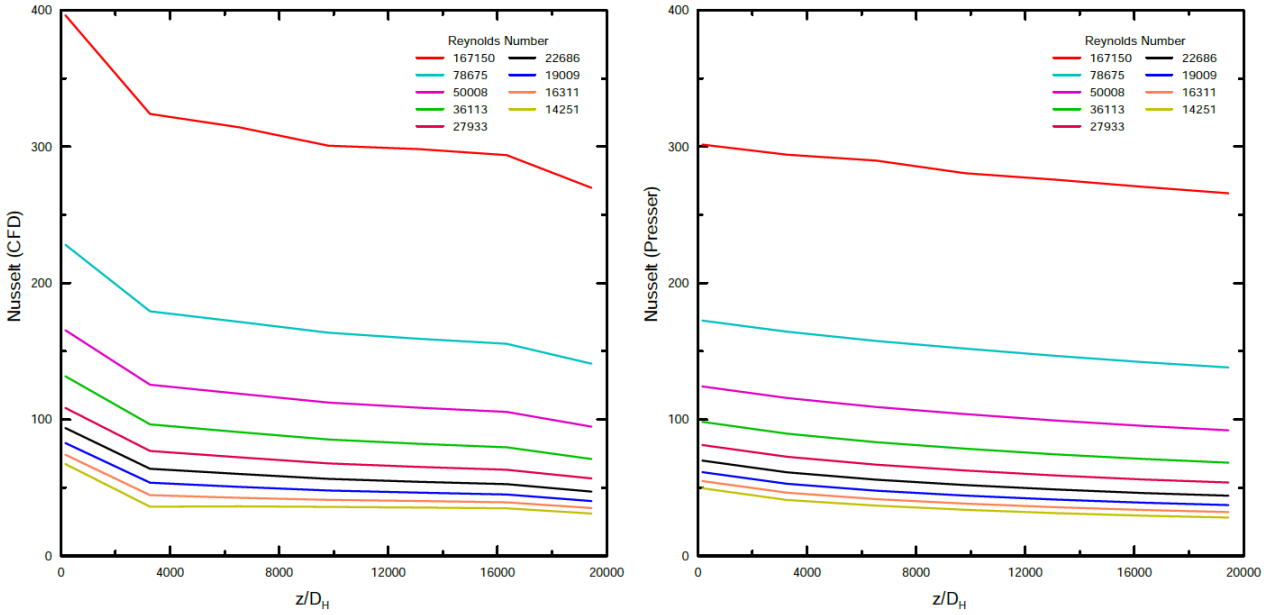

Figure 6. Comparison between Nusselt numbers calculated by CFD and with the Presser correlation as a function of the dimensionless axial position.

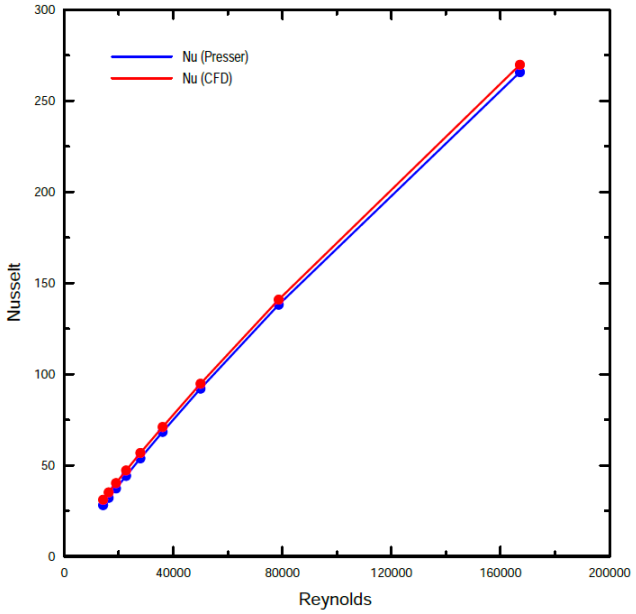

Figure 7. Nusselt number as a function of Reynolds number.

6. ACKNOWLEDGEMENTS

The authors acknowledge CNPq and FAPERJ for their financial support.

7. REFERENCES

Bovard, S., Abdi, M., Nikou, M.R.K. and Daryasafar, A., 2017. "Numerical investigation of heat transfer in supercritical CO_2 and water turbulent flow in circular tubes". *The Journal of Supercritical Fluids*, Vol. 119, pp. 81–103.

Bruch, A., Bontemps, A. and Colasson, S., 2009. "Experimental investigation of heat transfer of supercritical carbon dioxide flowing in a cooled vertical tube". *International Journal of Heat and Mass Transfer*, Vol. 51, pp. 2489–2598.

Duffey, R.B. and Pioro, I.L., 2005. "Experimental heat transfer of supercritical carbon dioxide flowing inside channels (survey)". *Nuclear Engineering and Design*, Vol. 235, pp. 913–924.

Fatima, R., 2010. *Numerical investigation of thermal hydraulic behavior of supercritical carbon dioxide in compact heat exchangers*. Ph.D. thesis, Texas AM University, Texas, USA.

Kim, D.E. and Kim, M.H., 2010. "Experimental study of the effects of flow acceleration and buoyancy on heat transfer in a supercritical fluid flow in a circular tube". *Nuclear Engineering and Design*, Vol. 240, pp. 3336–3349.

Menter, F.R., 1994. "Two-equation eddy-viscosity turbulence models for engineering applications". *AIAA Journal*, Vol. 32.

NIST, 2017. "Thermophysical properties of fluid systems". National Institute of Standards and Technology, 2017 <http://webbook.nist.gov/chemistry/fluid >.

Ross, S.B., El-Genk, M.S. and Matthews, R.B., 1988. "Thermal conductivity correlation for uranium nitride fuel between 10 and 1923 k". *Journal of Nuclear Materials*, Vol. 151, pp. 313–317.

Takahashi, Y., Murabayashi, M., Akimoto, Y. and Mukaibo, T., 1971. "Uranium mononitride: heat capacity and thermal conductivity from 298 to 1000 k". *Journal of Nuclear Materials*, Vol. 38, pp. 303–308.

Todreas, N.E. and Kazimi, M.S., 1990. *Nuclear Systems I*. Taylor & Francis, New York, USA.

Vieira, C.B., 2014. *"Simulação computacional de convecção natural turbulenta em cavidades com geração de calor volumétrica"*. Ph.D. thesis, COPPE/UFRJ, Rio de Janeiro, Brazil.

Wilcox, D.C., 2008. "Formulation of the k-omega turbulence model revisited". *AIAA Journal*, pp. 2823–2838.

Yu, H., Hartanto, D., Moon, J. and Kim, Y., 2015. "A conceptual study of a supercritical co2-cooled". *Energies*, Vol. 8, pp. 13938–13952.

8. RESPONSIBILITY NOTICE

The authors are the only responsibles for the printed material included in this paper.